PROCEEDINGS OF SCIENCE

Improving electron/proton discrimination at high energies with CALET on the International Space Station

Sandro Gonzi,[a,b,c,*] **Eugenio Berti,**[b,c] **Pietro Betti**[b,c] **and Lorenzo Pacini**[b,c] **for the CALET collaboration**

[a] *University of Florence, Department of Physics and Astronomy, Via Giovanni Sansone 1, 50019 Sesto Fiorentino, Italy*

[b] *National Institute for Nuclear Physics INFN, Division of Florence, Via Bruno Rossi 1, 50019 Sesto Fiorentino, Italy*

[c] *National Research Council CNR, Institute of Applied Physics IFAC, Via Madonna del Piano 10, 50019 Sesto Fiorentino, Italy*

E-mail: sandro.gonzi@unifi.it

The CALorimetric Electron Telescope (CALET), operating aboard the International Space Station since October 2015, is an experiment dedicated to high-energy astroparticle physics. The primary scientific goal of the experiment is the measurement of the electron+positron flux up to the multi-TeV region. At such high energies, proton contamination - coupled with limited statistics - is the main challenge for this measurement and good electron/proton discrimination can be carried out by using machine learning techniques. So far, we have tested and used only algorithms implemented in the ROOT TMVA package: in particular, the Boosted Decision Tree (BDT) algorithm leads to proton contamination below 10% up to 7.5 TeV with an 80% electron efficiency. In principle, better performance can be achieved by using Python packages, which offer a larger variety of machine learning algorithms and tuning parameters compared to TMVA. In this work, we will present a comparison of the performance obtained with the BDT algorithm implemented in TMVA and Python (XGBoost), while alternative approaches based on neural networks (e.g., Keras) will be explored in future studies.

39th International Cosmic Ray Conference (ICRC2025)
15–24 July 2025
Geneva, Switzerland

*Speaker

PoS(ICRC2025)011

1. Introduction

High-energy cosmic-ray electrons and positrons offer a valuable window into nearby astrophysical sources. Above 1 TeV, these particles suffer substantial energy losses during propagation, limiting their origin within about 1 kpc of the Solar System. Consequently, only a handful of local sources located in the proximity of the Solar System, such as nearby supernova remnants and pulsars, can contribute significantly to the observed flux at these energies.

Moreover, the apparent rise in the positron fraction above 10 GeV, as reported by the Payload for Antimatter Matter Exploration and Light nuclei Astrophysics (PAMELA) [1] and the Alpha Magnetic Spectrometer (AMS-02) [2] experiments, has spurred considerable interest in potential positron sources, whether of astrophysical origin (e.g., pulsars) or more exotic ones like dark matter annihilation or decay. Precise measurements of the inclusive (all-electron) spectrum at TeV energies could reveal features, such as spectral bumps or cutoffs, that help constrain the nature and distribution of these supposed sources.

The CALorimetric Electron Telescope (CALET) [3], installed on the International Space Station (ISS) since October 2015, is specifically designed for long-term observations of high-energy cosmic rays. Over recent years, CALET has provided direct measurements of the energy spectra of electrons and positrons up to 7.5 TeV [4–6], protons up to 60 TeV [7, 8], helium nuclei up to 250 TeV [9], as well as heavier nuclei such as boron, carbon, oxygen, iron and nickel [10–13].

This work presents a study focused on the measurement of the all-electron spectrum in the TeV range using multivariate analysis and machine learning techniques. These methods exploit variables related to shower development within the detector to improve electron/proton discrimination, which is particularly critical at high energies where the electron statistics become limited. Section 2 provides a brief overview of the CALET instrument. Section 3 outlines the employed multivariate and machine learning methods, while Section 4 presents the resulting performance and optimization outcomes. Finally, Section 5 summarizes the main findings of this work and outlines possible directions for future developments.

2. CALET Detector

CALET is a fully calorimetric instrument with a vertical thickness of 30 radiation lengths X_0 and 1.3 proton interaction lengths λ_I for particles at normal incidence. Its geometrical factor for high-energy electrons is approximately 1040 cm^2 sr, with a field of view extending to about 45° from zenith.

The detector is composed of three main subsystems. The CHarge Detector (CHD), positioned at the top, consists of two orthogonal layers of plastic scintillator hodoscopes and is used to identify the charge of incoming particles. Below the CHD is the Imaging Calorimeter (IMC), a fine-grained sampling calorimeter made of tungsten plates interleaved with layers of individually read-out scintillating fibers, providing detailed information on the early development of the shower. Finally, the Total AbSorption Calorimeter (TASC) is a thick, segmented calorimeter made of lead tungstate ($PbWO_4$), capable of fully containing the electromagnetic showers up to multi-TeV energies.

CALET also includes a dedicated gamma-ray burst monitor (CGBM), enabling complementary observations in gamma-ray astrophysics.

The overall instrument design enables CALET to achieve excellent energy resolution for electromagnetic showers ($\sim 2\%$ above 20 GeV) and a proton rejection power exceeding 10^5. These capabilities make it well-suited for precision measurements of the all-electron spectrum in the TeV range, even in the presence of a dominant proton background.

3. Proton Background Suppression via Multivariate Analysis

Monte Carlo (MC) simulations of electrons and protons, based on the EPICS framework [14], were employed to evaluate the key analysis components, including event selection and reconstruction efficiencies, energy corrections, and residual background contamination.

A first level of event pre-selection [15] is applied to isolate a clean sample of electron candidates. This step ensures that only well-reconstructed events within the geometrical acceptance are retained and that particles with charge $Z > 1$ are effectively excluded.

Following pre-selection, residual contamination from protons must be further suppressed using dedicated rejection methods. At energies below 500 GeV, a simple two-variable cut (the so-called K-cut) [15] provides a robust and efficient separation between electrons and protons. However, this approach becomes less effective in the TeV region, where the electron statistics are limited and the hadronic background is more pronounced.

To address this, a multivariate classification strategy is adopted for energies above 500 GeV. The classification tools are based on the Toolkit for Multivariate Analysis (TMVA) [16], which is integrated within the ROOT environment [17]. TMVA offers a suite of supervised machine learning algorithms, including decision trees, boosted classifiers, and neural networks. These methods are trained on labeled MC samples to learn the separation boundary between signal (all-electron) and background (protons), and then applied to the data to perform event classification. All multivariate techniques in TMVA make use of training events, for which the desired output is known, to determine the mapping function that describes a decision boundary (classification). Among the classification algorithms available in the TMVA toolkit, the application of the Boosted Decision Trees (BDT) has been chosen as a background-rejection algorithm for the CALET all-electron analysis with the goal of minimizing proton contamination (below 10% up to 7.5 TeV) while maintaining an electron selection efficiency of approximately 80%. In particular, the classical BDT approach has been proposed, by fixing some parameters as the minimum percentage of training events required in a leaf node (2.5%), the number of grid points in variable range used in finding optimal cut in node splitting (20), the boosting type for the trees in the forest (*Adaptive Boost* with a learning rate of 0.5%), the *bagging* resampling technique (with a sample fraction of 0.5%), the separation criterion for node splitting (*GiniIndex*). The number of trees in the forest ($t = 1000$) and the maximum depth of the decision tree allowed ($d = 5$) were chosen as part of a broader optimization process aimed at maximizing the overall classification performance. In figure 1 the Receiver Operating Characteristic (ROC) diagram, showing the background rejection versus the signal efficiency, is reported in the energy bin with $E \in [2899, 4594]$ GeV, for four tested methods available in the TMVA package: two BDT applications with different parameters, a MultiLayer Perceptrons (MLP) along with its bayesian extension referred to as MultiLayer Perceptrons Bayesian Neural Network (MLPBNN) and a Deep Neural Network (DNN) approach. This result justify the choice of the TMVA BDT ($t = 1000$, $d = 5$) as the reference algorithm in the CALET all-electron analysis [18].

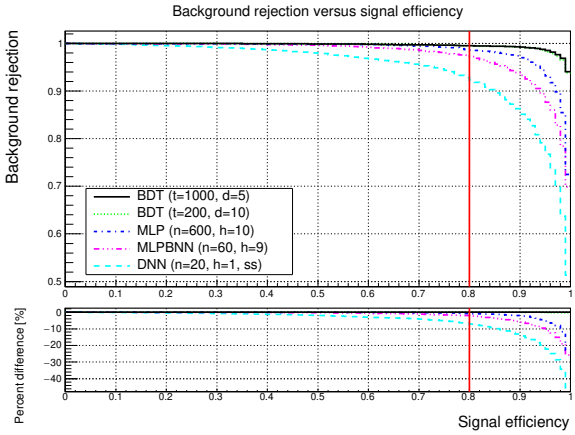

Figure 1: Receiver Operating Characteristic (ROC) diagram for the selected TMVA methods and percent difference with respect to the BDT ($t = 1000$, $d = 5$) one, chosen as the reference algorithm, in the energy bin with $E \in [2899, 4594]$ GeV. The vertical line indicates the 80% signal efficiency fixed in the analysis for the electron selection [18].

While TMVA provides a convenient and well-integrated framework for multivariate analysis within ROOT, it is somewhat limited in terms of algorithmic variety and flexibility in hyperparameter optimization. In principle, better performance can be achieved by using Python-based machine learning libraries, which offer a broader set of classification algorithms and more advanced tools for model tuning and validation. In this context, we present a comparative study between the BDT implementation in TMVA and that provided by the eXtreme Gradient Boosting (XGBoost) package [19] in Python, which is known for its efficiency and scalability. XGBoost is an optimized distributed gradient boosting library that implements machine learning algorithms under the Gradient Boosting framework, providing a parallel tree boosting also known as Gradient Boosted Decision Trees (GBDT). The most important factor behind the success of XGBoost is its scalability in all scenarios: the system runs more than ten times faster than existing popular solutions on a single machine and scales to billions of examples in distributed or memory-limited settings.

4. Results

Since the multivariate classification strategy is adopted for energies above 500 GeV, we limit the comparison between XGBoost GBDT and TMVA BDT performance in that energy region. The CALET all-electron analysis exploits the full geometrical acceptance of the instrument in this energy range, referred to as ABCD category. This includes the AB category, which consists of fully contained events, as well as category C, which accounts for events entering through the sides of the IMC, and category D, which includes events exiting through the lateral sides of the TASC [5].

To ensure a consistent comparison between the performance of the XGBoost GBDT and the TMVA BDT classifiers, the following conditions are imposed:

1. an identical electron selection efficiency of 80% is required for the background rejection cut;
2. the same set of input variables is used for training both classifiers. Specifically, 13 variables describing the longitudinal and transverse development of the shower within the CALET

calorimeter system are employed [15]. These observables were selected to maximize the separation power between electromagnetic and hadronic events, while preserving stability with respect to energy-dependent fluctuations;

3. the comparison is performed without applying any proton reweighting.

An important difference between the two approaches lies in how the Monte Carlo samples of all-electron and protons, selected after pre-selection cuts, are partitioned. For the TMVA BDT, the events were randomly divided into training and test sets using a fixed random seed, ensuring an equal number of events in each set within every energy bin. In the case of the XGBoost GBDT, the same random seed was used, but the dataset was instead split into three equally sized subsets: training, validation, and test sets.

The XGBoost algorithm optimizes a second-order approximation of the loss function. This approach ensures fast convergence and high classification accuracy, particularly suitable for imbalanced problems such as electron/proton separation at high energies. In this work, the loss function adopted is the logarithmic loss (log loss), which incorporates the uncertainty of predictions by penalizing incorrect classifications more severely when they are made with high confidence.

To prevent overfitting and improve generalization, early stopping was employed: training is halted if the validation loss does not improve after 10 consecutive boosting rounds. With this setup, no signs of overfitting were observed even after 100 boosting iterations.

Figure 2 shows the performance of the XGBoost algorithm evaluated in the deposited energy bin $E_{\text{Dep}} \in [728, 917]$ GeV.

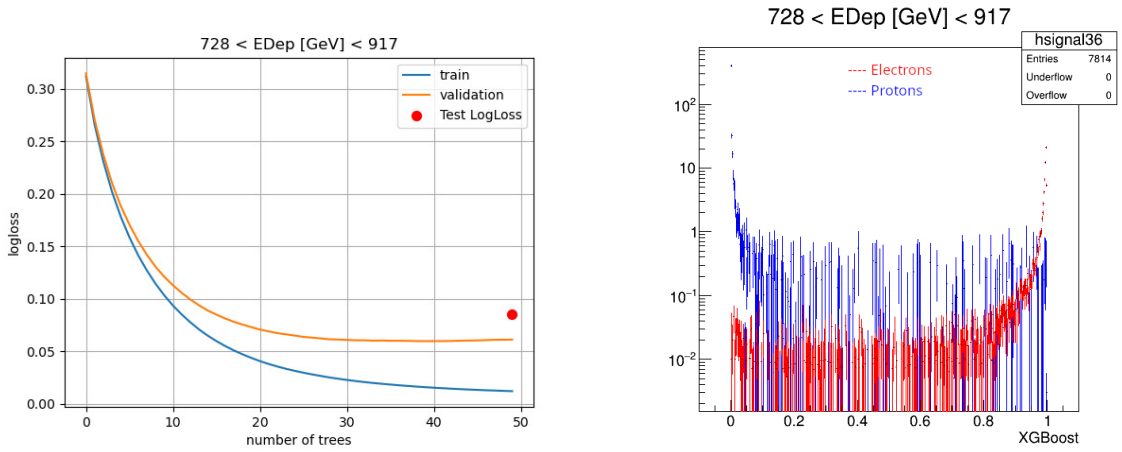

(a) **(b)**

Figure 2: performance of the XGBoost GBDT classifier evaluated in the deposited energy bin $E_{\text{Dep}} \in [728, 917]$ GeV. **(a)** Log loss as a function of the number of trees. The training and validation profile are reported together with the test value. **(b)** XGBoost distribution for electrons and protons.

The log loss as a function of the number of trees, evaluated in the selected energy bin, is shown in figure 2a. The plot clearly illustrates that the training and validation curves remain well separated, with the validation loss reaching a plateau after approximately 30 iterations, indicating a reduced risk of overfitting. The figure also reports the corresponding log loss value for the test

sample, providing an independent measure of the classifier's generalization performance. Figure 2b shows the XGBoost output distribution in the same energy range for the test sample, highlighting the effective separation between signal and background.

Figure 3 presents the contamination, quantified as the background-to-signal ratio remaining after proton suppression using multivariate classification techniques. The plot compares the performance of the XGBoost GBDT classifier, evaluated on training, validation, and test samples, with that of the TMVA BDT across different bins of reconstructed energy E.

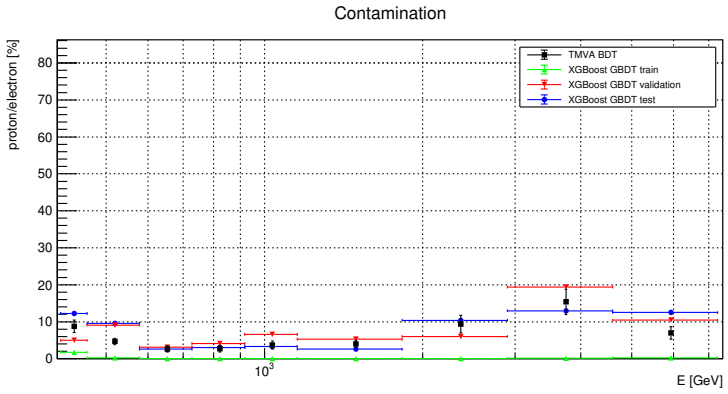

Figure 3: contamination in the reconstructed energy range $E \in [476, 7536]$ GeV.

The results indicate that, under the current configuration, XGBoost GBDT reproduces the performance of the standard TMVA BDT without yielding substantial improvements. This outcome highlights a critical limitation: at high energies, where statistics are low, splitting the Monte Carlo samples (surviving pre-selection) into training, validation, and test subsets results in reduced classification performance, particularly due to the scarcity of background events.

5. Conclusions

In this work, we presented a comparative study of proton background rejection in the CALET all-electron analysis using multivariate classification techniques. The standard Boosted Decision Tree algorithm implemented within the TMVA framework was compared to the Gradient Boosted Decision Tree approach provided by the XGBoost library in Python. Both methods were trained and evaluated on identical sets of input variables and MC samples, ensuring a fair comparison.

Results show that the XGBoost-based classification reproduces the performance of the TMVA implementation without introducing significant improvements. This suggests that, in the current configuration, the classifier's effectiveness is limited primarily by the statistics of the available MC samples, particularly at the highest energies, rather than by the choice of algorithm itself.

Future investigations could explore tuning the hyperparameters that were kept fixed in the current configuration, with the goal of optimizing performance while maintaining stability. Another promising approach involves redefining the binning used for background rejection studies, decoupling it from that of the pre-selection phase. This strategy would allow for improved statistical power in the high-energy regime, with the resulting contamination trends smoothed and regularized using analytical functions.

Additionally, some alternative approaches based on neural networks implemented using the Keras API [20] could be considered for further performance gains with the goal of assessing potential improvements in background rejection and classification robustness.

Acknowledgments

We gratefully acknowledge JAXA's contributions to the development of CALET and to the operations aboard the JEM-EF on the ISS. This work was supported in part by JSPS Grant-in-Aid for Scientific Research (S) No. 26220708, No. 19H05608, and No. 24H00025, JSPS Grant-in-Aid for Scientific Research (B) No. 24K00665, and by the MEXT Supported Program for the Strategic Research Foundation at Private Universities (2011-2015) (No. S1101021) at Waseda University. The CALET effort in Italy is supported by ASI under Agreement No. 2013-018-R.0 and its amendments. The CALET effort in the United States is supported by NASA through Grants No. NNX16AB99G, No. NNX16AC02G, and No. NNH14ZDA001N-APRA-0075.

References

[1] O. Adriani *et al.* (PAMELA Collaboration), *An anomalous positron abundance in cosmic rays with energies 1.5–100 GeV*, *Nature* **458** (2009) 607 [astro-ph/0810.4995].

[2] L. Accardo *et al.* (AMS Collaboration), *High Statistics Measurement of the Positron Fraction in Primary Cosmic Rays of 0.5–500 GeV with the Alpha Magnetic Spectrometer on the International Space Station*, *Phys. Rev. Lett.* **113** (2014) 121101.

[3] S. Torii, P. S. Marrocchesi *et al.* (CALET Collaboration), *The CALorimetric Electron Telescope (CALET) on the International Space Station*, *Adv. Space Res.* **64** (2019) 2531.

[4] O. Adriani *et al.* (CALET Collaboration), *Energy Spectrum of Cosmic-Ray Electron and Positron from 10 GeV to 3 TeV Observed with the Calorimetric Electron Telescope on the International Space Station*, *Phys. Rev. Lett.* **119** (2017) 181101 [astro-ph.HE/1712.01711].

[5] O. Adriani *et al.* (CALET Collaboration), *Extended Measurement of the Cosmic-Ray Electron and Positron Spectrum from 11 GeV to 4.8 TeV with the Calorimetric Electron Telescope on the International Space Station*, *Phys. Rev. Lett.* **120** (2018) 261102 [astro-ph.HE/1806.09728].

[6] O. Adriani *et al.* (CALET Collaboration), *Direct Measurement of the Spectral Structure of Cosmic-Ray Electrons+Positrons in the TeV Region with CALET on the International Space Station*, *Phys. Rev. Lett.* **131** (2023) 191001 [astro-ph.HE/2311.05916].

[7] O. Adriani *et al.* (CALET Collaboration), *Direct Measurement of the Cosmic-Ray Proton Spectrum from 50 GeV to 10 TeV with the Calorimetric Electron Telescope on the International Space Station*, *Phys. Rev. Lett.* **122** (2019) 181102 [astro-ph.HE/1905.04229].

[8] O. Adriani *et al.* (CALET Collaboration), *Observation of Spectral Structures in the Flux of Cosmic-Ray Protons from 50 GeV to 60 TeV with the Calorimetric Electron Telescope on the International Space Station*, *Phys. Rev. Lett.* **129** (2022) 101102 [astro-ph.HE/2209.01302].

[9] O. Adriani *et al.* (CALET Collaboration), *Direct Measurement of the Cosmic-Ray Helium Spectrum from 40 GeV to 250 TeV with the Calorimetric Electron Telescope on the International Space Station*, *Phys. Rev. Lett.* **130** (2023) 171002 [astro-ph.HE/2304.14699].

[10] O. Adriani *et al.* (CALET Collaboration), *Cosmic-Ray Boron Flux Measured from 8.4 GeV/n to 3.8 TeV/n with the Calorimetric Electron Telescope on the International Space Station*, *Phys. Rev. Lett.* **129** (2022) 251103 [astro-ph.HE/2212.07873].

[11] O. Adriani *et al.* (CALET Collaboration), *Direct Measurement of the Cosmic-Ray Carbon and Oxygen Spectra from 10 GeV/n to 2.2 TeV/n with the Calorimetric Electron Telescope on the International Space Station*, *Phys. Rev. Lett.* **125** (2020) 251102 [astro-ph.HE/2012.10319].

[12] O. Adriani *et al.* (CALET Collaboration), *Measurement of the Iron Spectrum in Cosmic Rays from 10 GeV/n to 2.0 TeV/n with the Calorimetric Electron Telescope on the International Space Station*, *Phys. Rev. Lett.* **126** (2021) 241101 [astro-ph.HE/2106.08036].

[13] O. Adriani *et al.* (CALET Collaboration), *Direct Measurement of the Nickel Spectrum in Cosmic Rays in the Energy Range from 8.8 GeV/n to 240 GeV/n with CALET on the International Space Station*, *Phys. Rev. Lett.* **128** (2022) 131103 [astro-ph.HE/2204.00845].

[14] K. Kasahara, *Introduction to Cosmos and some Relevance to Ultra High Energy Cosmic Ray Air Showers*, in proceedings of *24th International Cosmic Ray Conference (ICRC1995)*, Editrice Compositori, Bologna 1995.

[15] E. Berti *et al.* (CALET Collaboration), *The analysis strategy for the measurement of the electron flux with CALET on the International Space Station*, in proceedings of *37th International Cosmic Ray Conference (ICRC2021)*, PoS(ICRC2021)065 (2022).

[16] A. Hoecker *et al.*, *TMVA: Toolkit for Multivariate Data Analysis*, *CERN-OPEN-2007-007*, *arXiv:physics/0703039* [physics.data-an].

[17] R. Brun and F. Rademakers, *ROOT - An Object Oriented Data Analysis Framework*, in proceedings of *5th International Workshop on New Computing Techniques in Physics Research: Software Engineering, Neural Nets, Genetic Algorithms, Expert Systems, Symbolic Algebra, Automatic Calculations (AIHENP 96)*, *Nucl. Instrum. Meth. A* **389** (1997) 81.

[18] S. Gonzi *et al.* (CALET Collaboration), *Optimization of the proton background rejection in the measurement of the electron flux at high energies with CALET on the International Space Station*, in proceedings of *38th International Cosmic Ray Conference (ICRC2023)*, PoS(ICRC2023)090 (2024).

[19] T. Chen and C. Guestrin, *XGBoost: A Scalable Tree Boosting System*, in proceedings of *22nd ACM SIGKDD International Conference on Knowledge Discovery and Data Mining (KDD '16)*, pp. 785-794 (2016).

[20] F. Chollet *et al.*, *Keras* (2015), https://keras.io

Full Author List: CALET Collaboration

O. Adriani[1,2], Y. Akaike[3,4], K. Asano[5], Y. Asaoka[5], E. Berti[2,6], P. Betti[2,6], G. Bigongiari[7,8], W.R. Binns[9], M. Bongi[1,2], P. Brogi[7,8], A. Bruno[10], N. Cannady[11], G. Castellini[6], C. Checchia[7,8], M.L. Cherry[12], G. Collazuol[13,14], G.A. de Nolfo[10], K. Ebisawa[15], A.W. Ficklin[12], H. Fuke[15], S. Gonzi[1,2,6], T.G. Guzik[12], T. Hams[16], K. Hibino[17], M. Ichimura[18], M.H. Israel[9], K. Kasahara[19], J. Kataoka[20], R. Kataoka[21], Y. Katayose[22], C. Kato[23], N. Kawanaka[24,25], Y. Kawakubo[26], K. Kobayashi[3,4], K. Kohri[25,27], H.S. Krawczynski[9], J.F. Krizmanic[11], P. Maestro[7,8], P.S. Marrocchesi[7,8], M. Mattiazzi[13,14], A.M. Messineo[8,28], J.W. Mitchell[11], S. Miyake[29], A.A. Moiseev[11,30,31], M. Mori[32], N. Mori[2], H.M. Motz[33], K. Munakata[23], S. Nakahira[15], J. Nishimura[15], M. Negro[12], S. Okuno[17], J.F. Ormes[34], S. Ozawa[35], L. Pacini[2,6], P. Papini[2], B.F. Rauch[9], S.B. Ricciarini[2,6], K. Sakai[36], T. Sakamoto[26], M. Sasaki[11,30,31], Y. Shimizu[17], A. Shiomi[37], P. Spillantini[1], F. Stolzi[7,8], S. Sugita[26], A. Sulaj[7,8], M. Takita[5], T. Tamura[17], T. Terasawa[5], S. Torii[3], Y. Tsunesada[38,39], Y. Uchihori[40], E. Vannuccini[2], J.P. Wefel[12], K. Yamaoka[41], S. Yanagita[42], A. Yoshida[26], K. Yoshida[19], and W.V. Zober[9]

[1]Department of Physics, University of Florence, Via Sansone, 1 - 50019, Sesto Fiorentino, Italy, [2]INFN Sezione di Firenze, Via Sansone, 1 - 50019, Sesto Fiorentino, Italy, [3]Waseda Research Institute for Science and Engineering, Waseda University, 17 Kikuicho, Shinjuku, Tokyo 162-0044, Japan, [4]Space Environment Utilization Center, Human Spaceflight Technology Directorate, Japan Aerospace Exploration Agency, 2-1-1 Sengen, Tsukuba, Ibaraki 305-8505, Japan, [5]Institute for Cosmic Ray Research, The University of Tokyo, 5-1-5 Kashiwa-no-Ha, Kashiwa, Chiba 277-8582, Japan, [6]Institute of Applied Physics (IFAC), National Research Council (CNR), Via Madonna del Piano, 10, 50019, Sesto Fiorentino, Italy, [7]Department of Physical Sciences, Earth and Environment, University of Siena, via Roma 56, 53100 Siena, Italy, [8]INFN Sezione di Pisa, Polo Fibonacci, Largo B. Pontecorvo, 3 - 56127 Pisa, Italy, [9]Department of Physics and McDonnell Center for the Space Sciences, Washington University, One Brookings Drive, St. Louis, Missouri 63130-4899, USA, [10]Heliospheric Physics Laboratory, NASA/GSFC, Greenbelt, Maryland 20771, USA, [11]Astroparticle Physics Laboratory, NASA/GSFC, Greenbelt, Maryland 20771, USA, [12]Department of Physics and Astronomy, Louisiana State University, 202 Nicholson Hall, Baton Rouge, Louisiana 70803, USA, [13]Department of Physics and Astronomy, University of Padova, Via Marzolo, 8, 35131 Padova, Italy, [14]INFN Sezione di Padova, Via Marzolo, 8, 35131 Padova, Italy, [15]Institute of Space and Astronautical Science, Japan Aerospace Exploration Agency, 3-1-1 Yoshinodai, Chuo, Sagamihara, Kanagawa 252-5210, Japan, [16] Center for Space Sciences and Technology, University of Maryland, Baltimore County, 1000 Hilltop Circle, Baltimore, Maryland 21250, USA, [17]Kanagawa University, 3-27-1 Rokkakubashi, Kanagawa, Yokohama, Kanagawa 221-8686, Japan, [18]Faculty of Science and Technology, Graduate School of Science and Technology, Hirosaki University, 3, Bunkyo, Hirosaki, Aomori 036-8561, Japan, [19]Department of Electronic Information Systems, Shibaura Institute of Technology, 307 Fukasaku, Minuma, Saitama 337-8570, Japan, [20]School of Advanced Science and Engineering, Waseda University, 3-4-1 Okubo, Shinjuku, Tokyo 169-8555, Japan, [21] Okinawa Institute of Science and Technology, 1919-1 Tancha, Onna-son, Kunigami-gun Okinawa 904-0495, Japan, [22]Faculty of Engineering, Division of Intelligent Systems Engineering, Yokohama National University, 79-5 Tokiwadai, Hodogaya, Yokohama 240-8501, Japan, [23]Faculty of Science, Shinshu University, 3-1-1 Asahi, Matsumoto, Nagano 390-8621, Japan, [24]Department of Physics, Graduate School of Science, Tokyo Metropolitan University , 1-1 Minamii-Osawa, Hachioji, Tokyo 192-0397, Japan, [25]National Astronomical Observatory of Japan, 2-21-1 Osawa, Mitaka, Tokyo 181-8588, Japan, [26]Department of Physical Sciences, College of Science and Engineering, Aoyama Gakuin University, 5-10-1 Fuchinobe, Chuo, Sagamihara, Kanagawa 252-5258, Japan, [27]Institute of Particle and Nuclear Studies, High Energy Accelerator Research Organization, 1-1 Oho, Tsukuba, Ibaraki 305-0801, Japan, [28]University of Pisa, Polo Fibonacci, Largo B. Pontecorvo, 3 - 56127 Pisa, Italy, [29]Department of Electrical and Electronic Systems Engineering, National Institute of Technology (KOSEN), Gifu College, 2236-2 Kamimakuwa, Motosu-city, Gifu 501-0495, Japan, [30]Center for Research and Exploration in Space Sciences and Technology, NASA/GSFC, Greenbelt, Maryland 20771, USA, [31]Department of Astronomy, University of Maryland, College Park, Maryland 20742, USA, [32]Department of Physical Sciences, College of Science and Engineering, Ritsumeikan University, Shiga 525-8577, Japan, [33]Faculty of Science and Engineering, Global Center for Science and Engineering, Waseda University, 3-4-1 Okubo, Shinjuku, Tokyo 169-8555, Japan, [34]Department of Physics and Astronomy, University of Denver, Physics Building, Room 211, 2112 East Wesley Avenue, Denver, Colorado 80208-6900, USA, [35]Quantum ICT Advanced Development Center, National Institute of Information and Communications Technology, 4-2-1 Nukui-Kitamachi, Koganei, Tokyo 184-8795, Japan, [36]Kavli Institute for Cosmological Physics, The University of Chicago, 5640 South Ellis Avenue, Chicago, IL 60637, USA, [37]College of Industrial Technology, Nihon University, 1-2-1 Izumi, Narashino, Chiba 275-8575, Japan, [38]Graduate School of Science, Osaka Metropolitan University, Sugimoto, Sumiyoshi, Osaka 558-8585, Japan, [39]Nambu Yoichiro Institute for Theoretical and Experimental Physics, Osaka Metropolitan University, Sugimoto, Sumiyoshi, Osaka 558-8585, Japan, [40]National Institutes for Quantum and Radiation Science and Technology, 4-9-1 Anagawa, Inage, Chiba 263-8555, Japan, [41]Nagoya University, Furo, Chikusa, Nagoya 464-8601, Japan, [42]College of Science, Ibaraki University, 2-1-1 Bunkyo, Mito, Ibaraki 310-8512, Japan.